Design and Characterization of Helical Peptides that Inhibit the E6 Protein of Papillomavirus[†,‡]

Yuqi Liu,[§] Zhiguo Liu,[||,⊥] Elliot Androphy,[||] Jason Chen,[||] and James D. Baleja*[,§]

Department of Biochemistry, Tufts University School of Medicine, 136 Harrison Avenue, Boston, Massachusetts 02111, and Department of Medicine, University of Massachusetts Medical School, 55 Lake Avenue North, Worcester, Massachusetts 01605

Received March 5, 2004; Revised Manuscript Received April 9, 2004

ABSTRACT: The E6 protein from HPV type 16 binds proteins containing a seven-residue leucine-containing motif. Previous work demonstrated that peptides containing the consensus sequence are a mixture of α-helix and unstructured conformations. To design monomeric E6-binding peptides that are stable in aqueous solution, we used a protein grafting approach where the critical residues of the E6-binding motif of E6-associated protein, E6AP, LQELLGE, were incorporated into exposed helices of two stably folded peptide scaffolds. One series was built using the third zinc finger of the Sp1 protein, which contains a C-terminal helix. A second series was built using a Trp-cage scaffold, which contains an N-terminal helix. The chimeric peptides had very different activities in out-competing the E6−E6AP interaction. We characterized the peptides by circular dichroism spectroscopy and determined high-resolution structures by NMR methods. The E6-binding consensus motif was found to be helical in the high-quality structures, which had backbone root-mean-square deviations of less than 0.4 Å. We have successfully grafted the E6-binding motif into two parent peptides to create ligands that have biological activity while preserving the stable, native fold of their scaffolds. The data also indicate that conformational change is common in E6-binding proteins during the formation of the complex with the viral E6 protein.

The E6 protein is an oncoprotein produced by the high-risk type of human papillomavirus (HPV)[1] (*1*). The papillomavirus is a small DNA tumor virus that infects epithelial cells and is strongly associated with the development of cervical cancer (*2*). The E6 protein from HPV type 16 (HPV-16, the prototype of high-risk HPV) is a 151 amino acid residue protein of unknown three-dimensional structure that contains two zinc-binding domains (*2*−*7*). E6 is thought to promote tumorigenesis by stimulating cellular degradation of the tumor suppressor p53 (*2*, *8*, *9*) through formation of a trimeric complex that includes the cellular 100 kDa E6-associated protein, E6AP. E6AP contains an internal E6-binding domain (amino acid residues 391−408) and a C-terminal Hect domain that confers ubiquitin-protein ligase activity that results in the specific ubiquitination and subsequent degradation of p53 (*9*). E6 protein displays a variety of other activities unrelated to E6AP-mediated p53 degradation through recognition of other cellular proteins, for example: E6bp (*10*), fibulin-1 (*11*), CBP/p300 (*12*), zyxin (*13*), MAGI-1 (*14*), hDLG (*15*), paxillin (*16*, *17*), AP-1, a clathrin adaptor protein (*18*), Bak (*19*, *20*), E6TP1 (*21*), Tyk2 (*22*), hScrib (*23*), and tumor necrosis factor R1 (*24*). E6 also interacts with DNA, as it can activate or repress several cellular or viral promoters (*6*, *25*).

Sequence comparison among several of the E6-interacting proteins, including E6AP, reveals a consensus sequence, LxxϕLsh, where L indicates the conserved leucine residues, ϕ is a hydrophobic residue (usually leucine), h is an amino acid residue with a side-chain capable of accepting hydrogen bonds (Asp, Glu, Asn, or Gln), s represents a small amino acid residue (Gly or Ala), and xx is a dipeptide where one of the residues is Asp, Glu, Asn, or Gln(*26*). Mutation of the conserved hydrophobic residues in the motif eliminates binding, whereas mutation of most other residues significantly reduces binding (*26*−*28*). Previous work using secondary structure predictions and structure determinations using NMR methods demonstrated that peptides containing the consensus sequence clearly have a tendency to form an α-helix (*26*, *27*, *29*). Experimental evidence indicated that these E6-binding peptides were mostly unstructured in aqueous solution and required the addition of cosolvents, such as trifluoroethanol (TFE), which is said to possibly mimic the presence of the binding partner (*30*).

In this paper, E6-binding peptides were designed to be stable in aqueous solution without the presence of stabilizing partners such as E6 protein or TFE. The minimal E6-binding consensus sequence was grafted into the single α-helix of

[†] Supported in part by NIH grant AI38001. Jason Chen was supported in part by the Cancer Research Foundation of America and NIH Grant CA92746.

[‡] Atomic coordinates have been deposited with the Research Collaboratory for Structural Bioinformatics Protein Databank, filenames 1RIK, 1RIM, and 1RIJ.

* To whom correspondence should be addressed: Phone: (617) 636-6872. Fax: (617) 636-2409. E-mail: jim.baleja@tufts.edu.

[§] Tufts University School of Medicine.

[||] University of Massachusetts.

[⊥] Current address: Department of Gastroenterology, Xijing Hospital, Xi'an, China, 710032.

[1] Abbreviations: CD, circular dichroism spectroscopy; DDM, distance difference matrix; HPV, human papillomavirus; GST, glutathione-S-transferase; MALDI, matrix-assisted laser desorption/ ionization; NOESY, nuclear Overhauser effect spectroscopy; PMSF, phenylmethanesulfonylfluoride; rms, root-mean-square; TFE, trifluoroethanol; TOCSY, total correlation spectroscopy.

10.1021/bi049552a CCC: $27.50 © 2004 American Chemical Society
Published on Web 05/19/2004

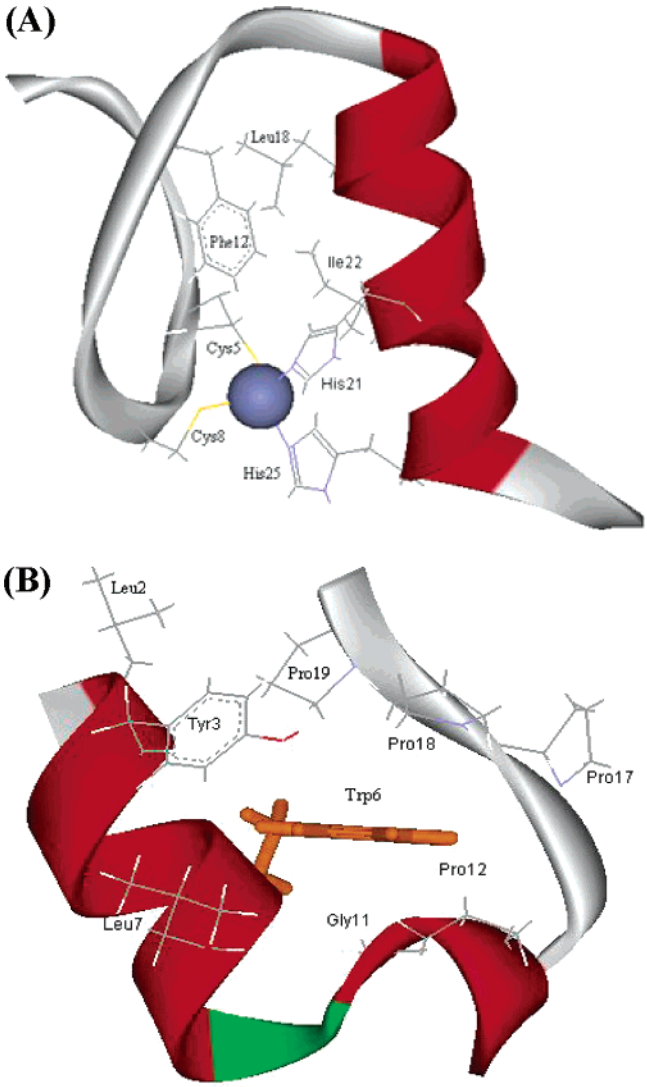

FIGURE 1: Two small stable peptide structures with exposed α-helices. (A) The structure of the third zinc-finger from the Sp1 protein (PDB accession code 1SP1). The 29-residue 1SP1 peptide contains an α-helix at its C-terminus (residues 16−25) (*41*). Side-chains are shown for residues important for ligating zinc and for stabilizing the hydrophobic core. (B) The structure of the Trp-cage peptide (PDB accession code 1L2Y). The 20-residue domain contains an α-helix at its N-terminus (residues 3−8) (*34*). Side-chains are indicated for the residues that stabilize the structural core of the peptide.

two different molecular scaffolds (Figure 1) and the generated peptides were tested to measure the extent to which they are biologically active. The solution structures of both active and inactive peptides were then determined by circular dichroism (CD) spectroscopy and nuclear magnetic resonance (NMR) methods. Correlation of the assay data with the structures provides insight into the mechanism of binding to the papillomavirus E6 protein and suggests that conformational change is common in E6-binding proteins during the formation of the complex. In the process, we have created ligands that have biological activity and retain the stable, native fold of the scaffold protein.

EXPERIMENTAL PROCEDURES

Peptide Synthesis. Each peptide was synthesized at the Tufts University Core Facility using Fmoc [*N*-(9-fluorenyl)-methoxycarbonyl] chemistry and contained an acetylated N-terminus and an amidated C-terminus. Peptides were purified by C_{18} reversed-phase high-performance liquid chromatography (HPLC), and identities were confirmed by matrix-assisted laser desorption/ionization (MALDI) mass spectrometry and by NMR spectroscopy.

In Vitro Association Assay. A fusion of E6AP with GST was prepared as described previously (*26*). Glutathione−Sepharose beads containing approximately 2 μg of GST−E6AP fusion protein were combined with 3 μL of ^{35}S-labeled in vitro-translated E6 protein in a total volume of 250 μL in a buffer containing 100 mM Tris-HCl (pH 8.0), 100 mM NaCl, 1% NP-40, 2 mM DTT, and 1 mM PMSF (phenylmethanesulfonylfluoride). Peptides were added at concentrations ranging from 0 to 100 μM. The mixtures were shaken gently for 3 h at 4 °C and then washed extensively with buffer, boiled in SDS-gel loading buffer, and electrophoresed on SDS-polyacrylamide gels. Gels were fixed, and intensities determined by densitometry. A plot of intensities versus peptide concentration was used to determine the concentration at which binding was reduced by 50% (Figure 2).

CD Spectroscopy. CD spectra were recorded in a 0.1 cm cuvette on a JASCO model 810 spectropolarimeter from 190 to 260 nm with two scans for all of the experiments. The bandwidth was 1 nm, and the scanning speed was 10 nm/min. The concentrations of the peptides were about 0.2 mM. E6apc1 and E6apc2 were in buffers containing 400 μM $ZnSO_4$ and 2 mM imidazole (pH 6.2), and E6apn1, E6apn2, and E6apm were in 5 mM phosphate buffer (pH 6.5). Thermal stability measurements were performed with incremental increases or decreases of 5 °C, and samples were equilibrated for 2 min at each temperature prior to data collection. Spectra were baseline-corrected by buffer subtraction. Helical content was estimated using CDNN2.1 (*31*).

NMR Spectroscopy. Samples of the E6apn1 and E6apn2 peptides were prepared at 5.0−6.0 mM concentration in double-distilled water with 10% D_2O and 20 μg/mL DSS as an internal standard. The pH was adjusted to 6.5. Samples of the E6apc1 and E6apc2 peptides, which were limited in quantity, were prepared at 1.2−3.0 mM concentration in buffers containing 10 mM deuterated imidazole, pH 6.0, 4 mM $ZnSO_4$, 1 mM deuterated DTT, 10% D_2O, and 20 μg/mL DSS. Samples in D_2O were prepared by lyophilizing the peptide solutions prepared in 90% H_2O/10% D_2O and redissolving in 99.96% D_2O. The pH values (direct meter readings) were the same as in the 90% H_2O/10% D_2O samples.

Spectra were collected at 25 °C on a Bruker AMX-500 spectrometer with a proton frequency of 500.14 MHz. Additional spectra for E6apn1 and E6apn2 were collected at 7 °C. Water suppression was performed by using presaturation. Two-dimensional NOESY, total correlation spectroscopy (TOCSY), and double-quantum-filtered COSY spectra were collected with 2048 points in t_2 and 512 time-proportional phase increments in t_1. Spectra were processed with shifted sine-bell window functions of about 60° (*32*). NOESY spectra were acquired with mixing times of 150 ms for the ∼30 residue peptides and 200 ms for the ∼25 residue peptides. TOCSY spectra were recorded with a mixing time of 57 ms using an MLEV-17 sequence (*32*). Final spectra were zero-filled to 4096 × 512 (real) points.

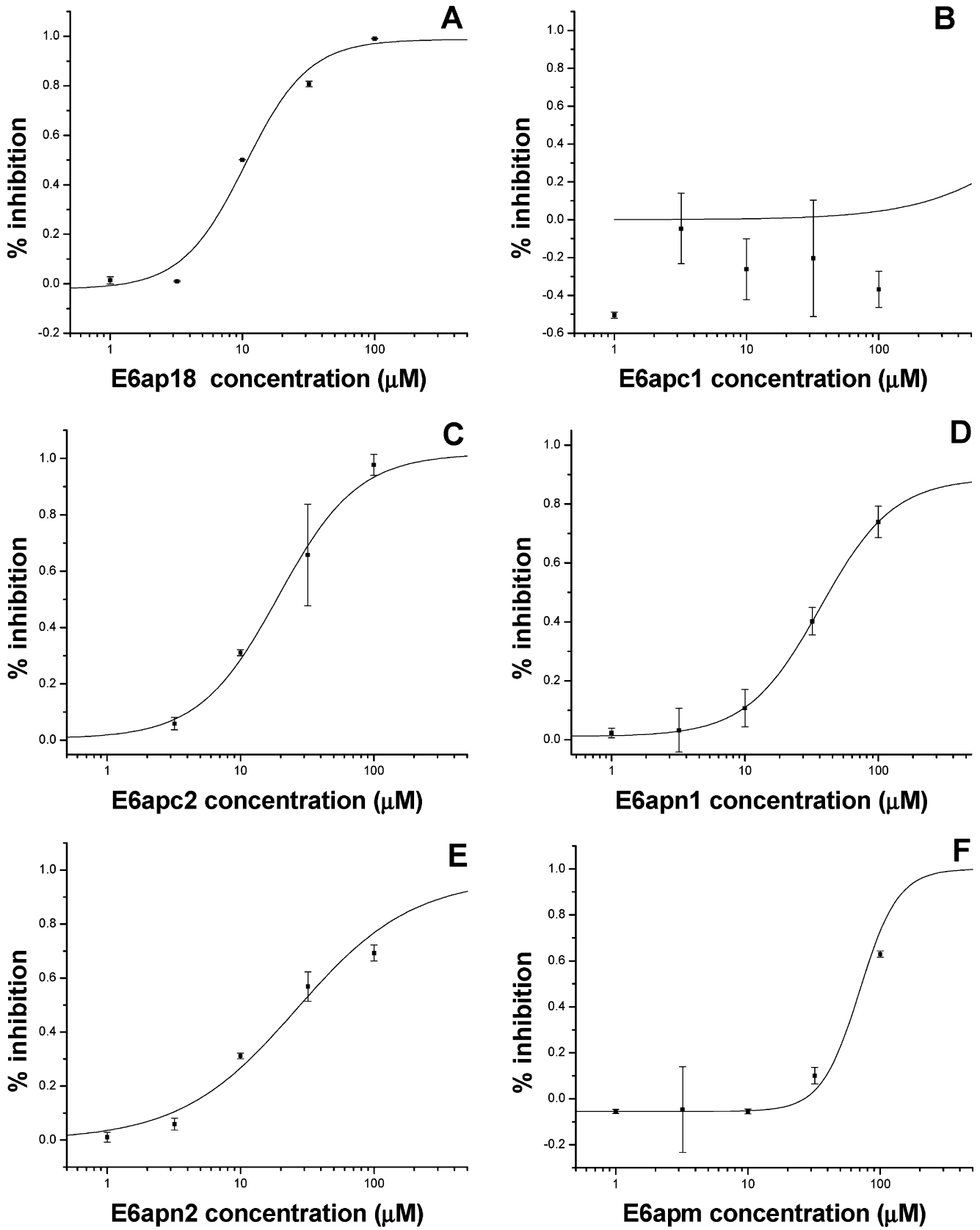

FIGURE 2: Inhibition of E6−E6ap interaction by the designed peptides. Experiments were performed in duplicate. (A) Inhibition by E6ap18 peptide. (B) Inhibition by E6apc1 peptide. (C) Inhibition by E6apc2 peptide. (D) Inhibition by E6apn1 peptide. (E) Inhibition by E6apn2 peptide. (F) Inhibition by E6apm. Data were fit using an equation modified from Sia et al. (*45*) $y = k/(1 + IC_{50}/x)$ (where k is a scaling factor, generally 1), except for the E6apc1 peptide, where the data were not fit, and a curve was drawn using an IC_{50} of 1000 μM.

Proton assignments were made by following standard homonuclear methods (*33*). The amino acid spin systems of E6apc1 and E6apc2 were assigned first from the TOCSY and double-quantum COSY spectrum to establish the intraresidue connectivity. Sequential assignment was then performed using the observed $d_{\alpha N}$, $d_{\beta N}$, and d_{NN} NOE cross-

Table 1: Peptide Sequences and Their E6-Inhibiting Activities[a]

name	sequence	IC_{50} (μM)
E6ap18	IPESS ELT**L**Q E**LL**GE ERR	10.5 ± 1.4
1SP1.pdb (1SP1 Zn finger)	KKFAC PECPK RFMRS *DHLSK HIKTH* QNKK	nd
E6apc1	YKFAC PECPK RFMRS DHLT**L** HI**LL**H ENKK	>1000
E6apc2	YKFAC PECPK RFMRS DHLSK HIT**L**H E**LL**GE ERR	19.3 ± 2.9
1L2Y.pdb (Trp-cage)	NL *YIQWL K*DGGP SSGRP PPS	nd
E6apn1	A**L**QE**L L**GQWL KDGGP SSGRP PPS	36.8 ± 3.2
E6apn2	A**L**QE**L L**GEYI QWLKD GGPSS GRPPP S	26.2 ± 4.8
E6apm	Y**L**QE**L L**GE	74.3 ± 1.9

[a] The three residues that, when mutated to alanine in the parent E6ap18 peptide, abolish binding to E6 are shown in bold. The E6ap18 peptide represents amino acid residues 391−408 of the E6-binding domain of E6AP protein (*26*). The E6apc series contains an E6-binding motif at the C-terminus of a zinc finger scaffold for which the helical residues are in italics (*41*). A third member of the series (E6apc3) containing the sequence KKFAC PECPK RFMRS DHLSK HI**L**QH **LL**GEK K had no activity for inhibiting the interaction of E6 with E6BP protein (unpublished results) and was not examined further. The E6apn1 and E6apn2 peptides contain the E6-binding motif at the N-terminus of a Trp-cage scaffold for which the helical residues are in italics (*34*). A peptide containing the minimal sequence for binding E6 (E6apm) was also tested. Peptides were assayed for their ability to inhibit the interaction of E6 with E6AP protein (see text for details).

peaks. Starting points for E6apn1 were based on the assignments of a similar peptide published by Neidigh et al. (*34*). Structure calculations were performed on monomers of E6apc1, E6apc2, and E6apn1 by employing the CNS program (version 1.1). The NOE and dihedral constraints were inputted using the default force constants (75 kcal/Å^2 and 400 kcal/deg^2, respectively). High-temperature dynamics, and then a cooling cycle in torsion space (with K_{NOE} = 150 kcal/mol), followed by further cooling in Cartesian space (K_{NOE} = 75 kcal/mol) and minimization (K_{NOE} = 75 kcal/mol), were performed with modifications as described (*35*). Briefly, (1) the cooling cycles in torsion space and in Cartesian space were each doubled in length. (2) The dihedral angle energy function was activated, and the chemical shift function was disabled. Then, (3) the E_{repel} function was replaced by a Lennard−Jones potential during the final Powell minimization. Ten accepted structures were accepted using the default ACCEPT script. Accepted structures were refined using the ENSEMBLE script with high-temperature dynamics and a cooling cycle in Cartesian space, followed by further cooling in Cartesian space. The number of the cooling cycles in Cartesian space was doubled, and the E_{repel} function was replaced by a Lennard−Jones potential during the final Powell minimization. Resulting structures were visualized by using MOLMOL 2K.1 (*36*).

RESULTS

To design E6-binding peptides that are stable, we chose a protein grafting approach where the critical residues of the E6-binding motif of E6AP, LQELLGE, were incorporated into an exposed helix of a stably folded peptide scaffold. The amino acid residues responsible for binding E6 form an α-helix but are conformationally labile when unbound (*26*, *37*), and it is expected that considerable entropy is lost on binding the E6 protein. Incorporation into a stable motif may reduce the entropic cost of binding and increase affinity. On the other hand, if the E6-binding motif is stabilized into the wrong conformation for binding, favorable binding enthalpy may be lost. In this "one-shot" grafting approach, our intent was to retain activity without significantly perturbing the structure of the protein host. We also desired that the resulting chimeric peptide not aggregate, thus remaining amenable to NMR spectroscopy, and that the residues that bind E6 be sufficiently dispersed for studies while bound to E6 protein. To date, no one has determined the structure of E6-binding peptide while bound to E6 or the structure of the peptide−E6 complex, mostly because the E6 protein is notoriously difficult to purify in quantities sufficient for NMR spectroscopy (*5*, *38*−*40*).

Although the predominant secondary structure of the E6-binding motif is helical, without the structure of the complex between peptide and E6, we do not know the extent of helix formation in detail. In particular, we are unsure of the conformation state (or states) of the glycine and glutamate residues at the C-terminal end of the motif or of adjacent residues external to the motif (*26*). In addition, the E6-binding pocket on E6 may also sterically exclude long helices, that is, an E6-binding motif that is contained within a long helix may not fit. Therefore, we investigated the use of two scaffolds that are expected to present exposed helices differently. One series, E6apc leaves the C-terminal end of the E6-binding motif exposed, whereas the other, E6apn, leaves the N-terminal end exposed.

The E6apc series was built on the scaffold of the third zinc finger of the Sp1 protein, which contains a C-terminal helix between residues Asp-16 and His-25 (*41*, *42*). While incorporating the E6-binding motif into the helix of the scaffold, several of the residues could not be modified, as they are important either for chelating the zinc ion (His-21 and His-25) or are part of the hydrophobic core of the zinc finger (e.g., Leu-18 and Ile-22). Other residues (16, 17, 19, 20, 23, and 24) appeared to be amenable to substitution. In the first construct, E6apc1, we substituted in leucines at positions 20, 23, and 24 to generate the motif LHILLHE. Although this motif lacked the glutamate immediately preceding the double-leucine and the small residue that follows the double-leucine that are conserved among E6-binding proteins, each can be substituted by alanine without loss of function (*27*). Other constructs (Table 1) moved the E6-binding motif toward the C-terminal end of the helix by one turn of helix. In one peptide, E6apc2, the generated motif was LHELLGE, containing a histidine predicted to be a helical residue that would also chelate the zinc ion.

A second series, E6apn, was built on a Trp-cage scaffold that was derived from the small peptide exendin-4 from Gila monster saliva and which contains an N-terminal helix from residues Tyr-3 to Lys-8 (*34*). Here, Trp-6 in the helix that is the core of the Trp-cage could clearly not be modified (Figure

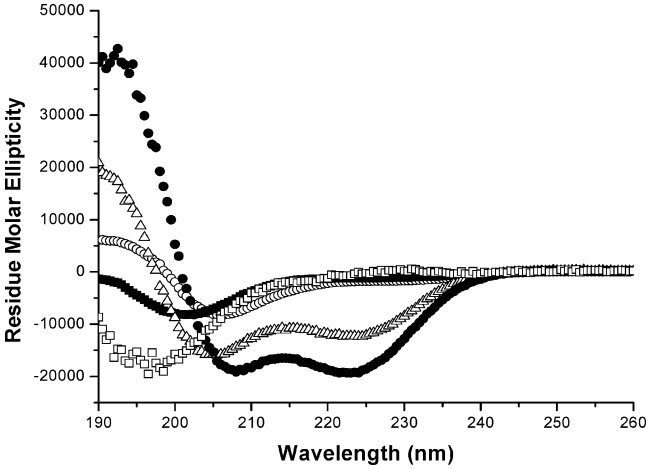

FIGURE 3: Circular dichroism spectroscopy of E6-binding peptides at room temperature. E6apc1, open circles; E6apc2, solid squares; E6apn1, open triangles; E6apn2, solid circles; E6apm, open squares. CD data were collected in 2 mM imidazole (pH 6.2) with 400 μM $ZnSO_4$ for E6apc1 and E6apc2 and in 5 mM phosphate (pH 6.5) for E6apn1, E6apn2, and E6apm.

1B). Other residues contributing to the hydrophobic core were Tyr-3 and Leu-7. On the other hand, Leu-2 appeared to point into the solution and was an excellent choice to be part of the E6-binding motif, LQELLGE. In the first construct, the tyrosine was changed to a leucine, and other changes were made resulting in a motif LQELLGQ. In the second construct, the E6-binding motif was shifted one turn of helix toward the N-terminus, thus retaining the tyrosine and resulting in the motif LQELLGE.

The peptides had very different activities in out-competing the E6−E6AP interaction (Figure 2 and Table 1). Inhibition by the E6apc2, E6apn1, E6apn2, and E6apm peptides was close to that of the parent 18mer peptide that we characterized previously (*26*), whereas E6apc1 did not show the inhibition. To understand the basis for why some peptides had activity while others did not, we wanted to know their three-dimensional structures.

We first examined the structures of the peptides using circular dichroism (CD) spectroscopy (Figure 3). The E6apn1 and E6apn2 peptides showed minima in their CD spectra at ∼207 and ∼224 nm and overall were very similar to that of the 20 amino acid residue Trp-cage scaffold reported by Neidigh et al. (*34*). The ellipticity at 222 nm for E6apn1 was ∼−12 500 deg cm^2 dmol^{-1}, whereas that of the Trp-cage scaffold was ∼−15 000 deg cm^2 dmol^{-1}, suggesting slightly less helical character. The ellipticity at 222 nm for E6apn2 was ∼−20 000 deg cm^2 dmol^{-1}, suggesting slightly more helical character. (The estimated percentages of α-helix in E6apn1 and E6apn2 are 35 and 62, respectively.) Our interpretation of these data is that at ambient temperatures, the E6apn1 peptide is less ordered in solution relative to the E6apn2 peptide. Compared to the E6apn peptides, E6apc1 and E6apc2 had less negative ellipticities at ∼207 nm and ∼222 nm and with a different ratio. The curve shape is similar to that of a single finger of TFIIIA (*43*) and three-finger domain of SP1 (*44*). Our interpretation of the E6apc data is that at ambient temperatures, the E6apc2 peptide may be less ordered in solution relative to the E6apc1 peptide. E6apm peptide, a short peptide containing only the residues needed for interaction with E6, was unstructured under the same conditions as evidenced by a minimum in the CD curve at 198 nm and an estimated secondary structure of 14% helix.

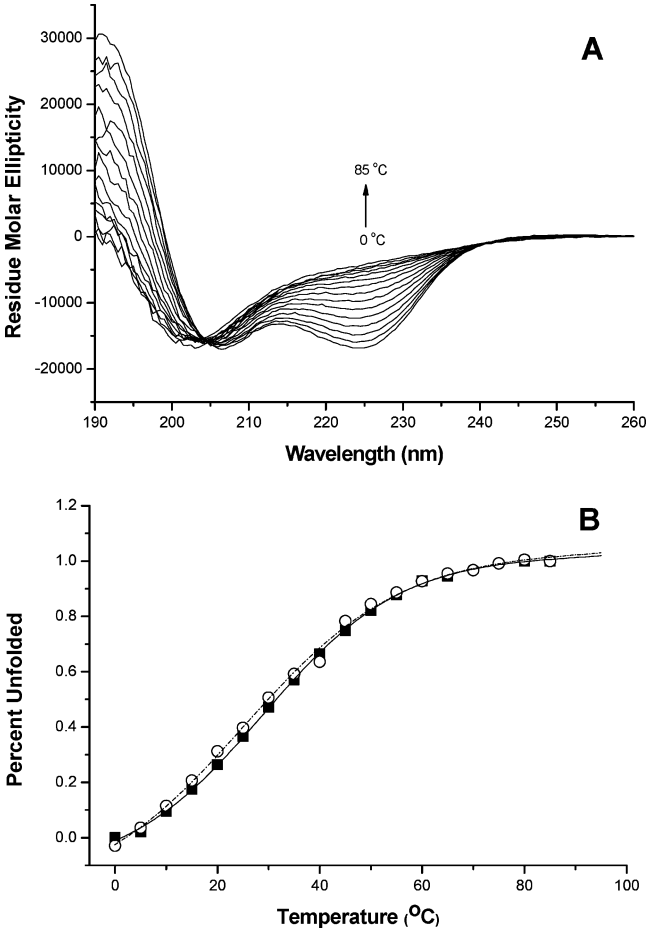

FIGURE 4: Thermal denaturation and renaturation of the E6apn1 peptide in 5 mM phosphate (pH 6.5). (A) CD spectra of the temperatures increasing from 0 and 65 °C in increments of 5 °C and a spectrum at 85 °C. (B) Thermal denaturation and renaturation profiles by monitoring the CD signal at 222 nm. Solid squares and the solid line indicate the denaturation profile, whereas open circles and the dashed line indicate the renaturation profile. The signal intensity was rescaled so that the reading at the highest temperature (85 °C) was 100% unfolded and the signal at 0 °C was 0% unfolded. Visual analysis resulted in a calculated T_m of 32 °C. If the peptide is partially unfolded at 0 °C, the calculated T_m is lower.

Because the peptides may change conformation on interaction with E6, we assessed the ability of each of the scaffolds to undergo conformational change using thermal denaturation. Thermal denaturation of a member of the E6apn series displayed reversible unfolding and folding with a T_m of about 32 °C (Figure 4). On the contrary, the CD spectrum of the zinc finger did not change significantly as a function of temperature (Figure 5). Because binding to E6 is likely to require changes in conformation (see discussion), the rigidity of the E6apc series suggests that there would be little loss of conformational entropy on binding (*45*), although too rigid a structure may exact a poor enthalpy of binding (*46*). The E6apn series seems to be the more promising scaffold for design.

Higher-resolution structures of the peptides were needed to assess residue-specific conformation and the details of the amino acid side-chains. One-dimensional ^{1}H NMR spectra of the E6apc1, E6apc2, and E6apn1 peptides displayed both good dispersion and narrow resonance lines, indicating that

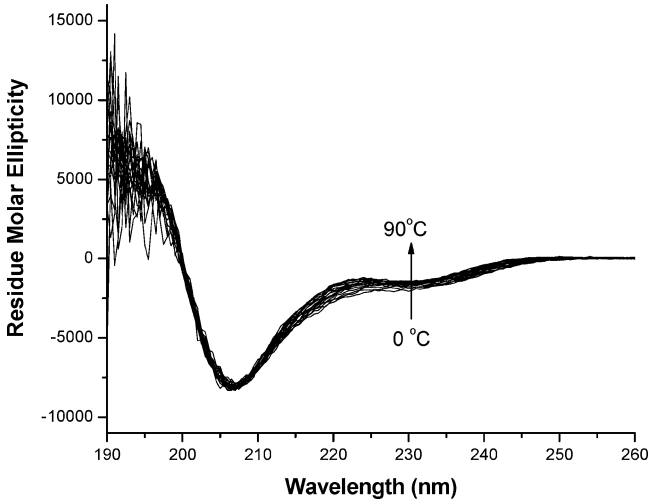

FIGURE 5: Thermal denaturation of the E6apc1 peptide in a buffer containing 400 μM $ZnSO_4$ and 2 mM imidazole (pH 6.2). CD spectra were collected at temperatures from 0 to 90 °C in increments of 5 °C.

the peptides folded well and that they would be good candidates for structure determination. The one- and two-dimensional NMR spectra of E6apn2 displayed good dispersion but broad peaks and weak intensity, suggesting aggregation at the high concentrations used for NMR, and the peptide was not analyzed further.

Resonance assignments were made by the usual strategy using two-dimensional TOCSY, double-quantum-filtered COSY, and NOESY spectra (*32*, *33*). The NOESY spectra of the three peptides E6apc1, E6apc2, and E6apn1 exhibited strong NOE cross-peaks between sequential residues in the amide−amide proton region typical of helix formation (Figures 1S−3S, Supporting Information). The α-protons of binding motif residues showed significant negative chemical shift deviation from random coil norms, indicating α-helical conformation both in the C-terminus of the E6apc peptides and in the N-terminus of the E6apn1 peptide (Figure 6) (*47*, *48*). Compared to other residues, the chemical shift deviation of Ser15 in E6apc1 and E6apc2 and that of Gly14 in E6apn1 are big. The large chemical shift deviation of Gly14 is primarily due to ring current shielding by Trp9. The deviation of Ser15 in E6apc1 and E6apc2 appears to be induced by the aromatic ring of Phe3.

For three-dimensional structure determination at atomic resolution, NOE cross-peak intensities were converted into distance restraints and calibrated using the covalently fixed distances of the well-ordered aromatic and histidine side-chains (*49*). The amide−amide distances in the helical regions were about 2.8 Å, indicating accurate calibration. The three-bond coupling constants, $^3J_{HN,H\alpha}$, were measured from the splitting of cross-peaks in the HN region of one-dimensional slices from a resolution-enhanced two-dimensional NOESY spectra of the spectra (*50*) and converted to dihedral angles (*51*). A small $^3J_{HN,H\alpha}$ (<6 Hz) value suggested that the corresponding ϕ angle was approximately −60° (±30); if $^3J_{HN,H\alpha}$ was large (>8.0 Hz), the ϕ angle was presumed to be −120°(±40). $^3J_{H\alpha,H\beta}$ values were measured from the splittings in the Hα dimension of the spectra collected in D_2O solution. At this stage, most of the β- and γ-methylene protons were also stereospecifically assigned on the basis of coupling constants and NOE patterns (Tables

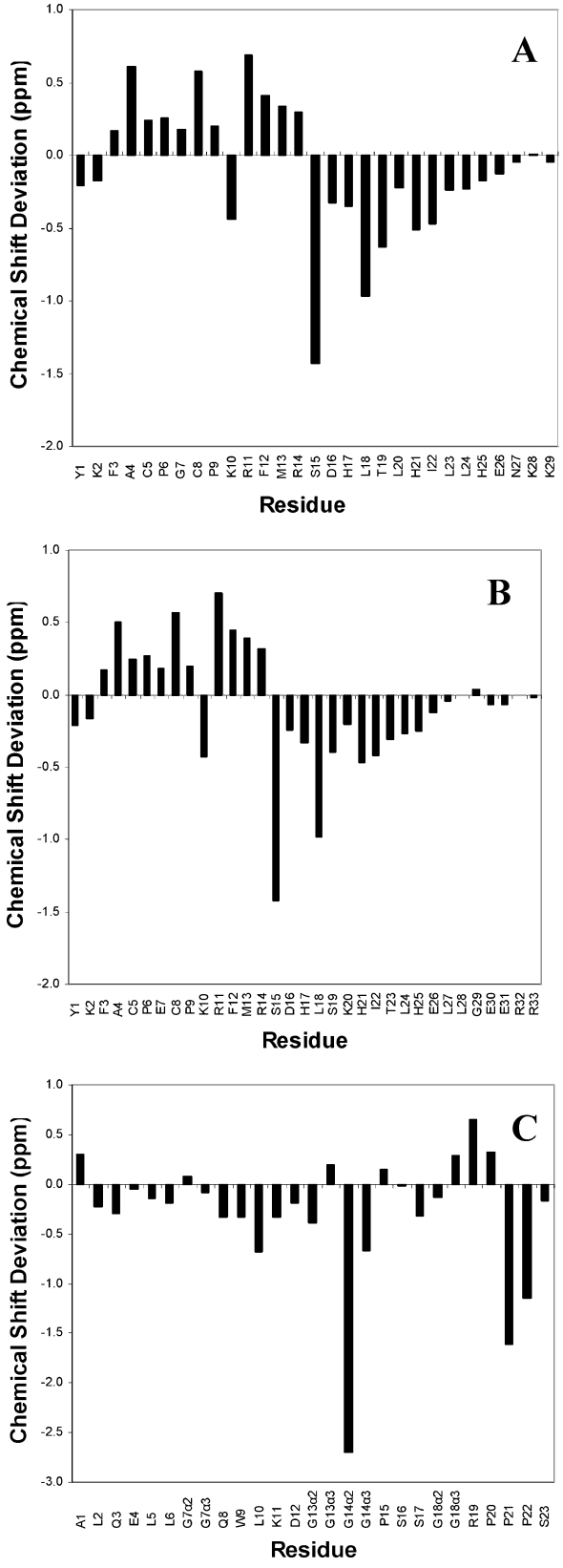

FIGURE 6: Chemical shift analysis of the E6-binding peptides. The chemical shifts of the Hα protons were compared to random coil values (*33*). Positive values are indicative of β-sheet formation, whereas consecutive negative values are indicative of an α-helix. (A) Analysis for E6apc1. (B) Analysis for E6apc2. (C) Analysis for E6apn1. In (C), the spectroscopically distinguishable α-protons of the four glycines are marked α2 and α3.

S1−S3, Supporting Information). Approximately 300 conformational restraints were obtained for each peptide (Table

Table 2: NMR Structural Data and Refinement Statistics

	E6apc1	E6apc2	E6apn1
experimental restraints			
distance restraints from NOEs	334	281	280
dihedral angle restraints	37	32	14
total no. of experimental restraints	371	313	294
rms deviations from experimental data			
average distance restraint violation (Å)	0.039 ± 0.001	0.043 ± 0.002	0.030 ± 0.001
distance restraint violations >0.5 Å	0.0 ± 0.0	0.0 ± 0.0	0.0 ± 0.0
average dihedral angle restraint violation (deg)	0.07 ± 0.03	0.09 ± 0.06	0.01 ± 0.03
dihedral angle restraint violations > 5°	0.0 ± 0.0	0.0 ± 0.0	0.0 ± 0.0
rms deviations from ideal stereochemistry			
bonds (Å)	0.0033 ± 0.0001	0.0035 ± 0.0001	0.0032 ± 0.0001
angles (deg)	0.470 ± 0.009	0.493 ± 0.009	0.500 ± 0.007
impropers (deg)	0.340 ± 0.019	0.285 ± 0.019	0.281 ± 0.013
Ramachandran analysis of the structures			
residues in favored regions	91.4%	74.4%	93.7%
residues in additionally allowed regions	8.6%	24.5%	6.3%
residues in generously allowed regions	0.1%	1.1%	0.0%
residues in disallowed regions	0.0%	0.0%	0.0%
Lennard−Jones potential energies			
after annealing (kcal mol^{-1})	−3.7 ± 10.3	−20.5 ± 11.6	−39.1 ± 5.1
ensemble average (kcal mol−1)	−32.1 ± 7.1	−38.2 ± 9.2	−40.8 ± 3.9
coordinate precision (Å)[a]			
backbone	0.37 ± 0.13	0.27 ± 0.10	0.32 ± 0.10
all heavy atoms	1.29 ± 0.21	1.06 ± 0.18	1.18 ± 0.19

[a] After superimposition of residues 3−26 of E6apc1, 3−25 of E6apc2, and 3−20 of E6apn1.

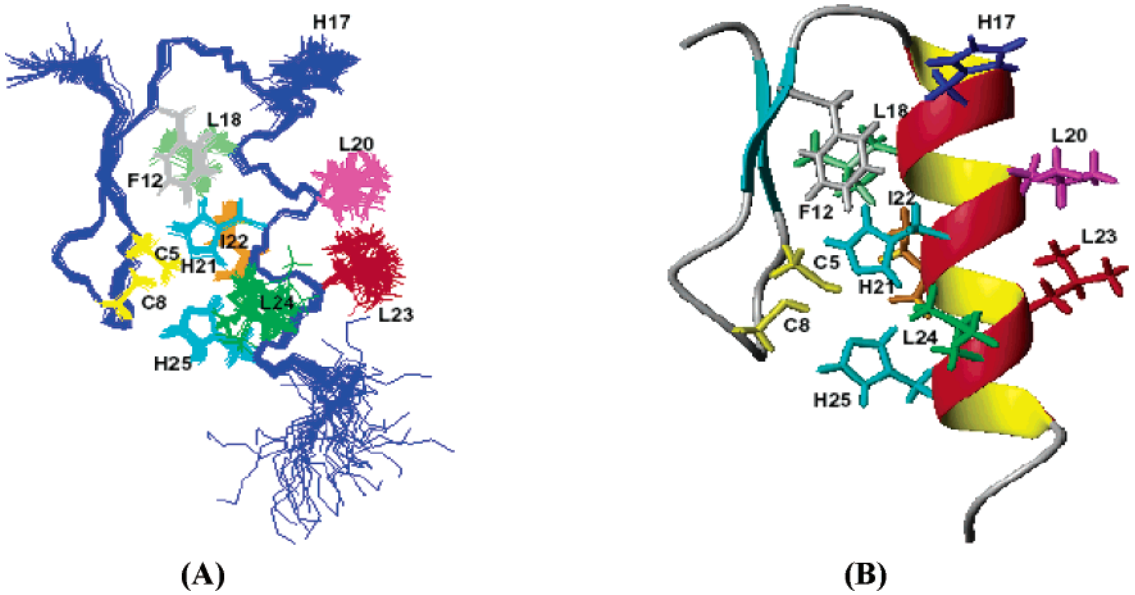

FIGURE 7: Three-dimensional structure of the E6apc1 peptide. (A) Bundle of 43 structures superimposed on the backbone atoms of residues from Phe3 to Glu26. (B) Randomly chosen structure. Side-chains are labeled for residues important for forming a stable core (Cys5 and Cys8 are yellow; His21 and His25 are cyan; Phe12 is gray; Leu18 is pale green) or for binding to E6 (Leu20, 23, and 24 are magenta, red, and green, respectively).

2) and were input into CNS for structure calculation. The constraints and the resulting statistical analysis of the final structures are shown in Table 2. The structures are of high quality. The total energies are low (about −36 kcal/mol), and the backbone rms deviations of superimposed structures are between 0.27 and 0.37 Å.

The E6apc1 peptide possesses the predicted conformation of a zinc finger motif (Figure 7). Four residues (Cys5, Cys8, His21, and His25) chelate one Zn^{2+}, and Phe12 and Leu18 form a hydrophobic core that stabilizes the conformation of the motif. Residues Phe3 to Ala4 and residues Arg11 to Phe12 form a small antiparallel β-sheet, and residues 15 to 26 form an α-helix. The three residues likely to be most important for binding E6 (Leu20, Leu23, and Leu24) are located in the middle of the helix, and their amide hydrogens participate in the hydrogen bonds associated with helices. Their side-chains extend into the solvent away from the portion of the peptide structure that forms the small β-sheet.

The E6apc2 peptide shows the same overall conformation (Figure 8), except that the α-helix was between residues 15 and 25. Only the first leucine residue (Leu24) of the assumed E6-binding motif is located in the well-defined helix, the second and third leucine residues, Leu27 and Leu28, respectively, are outside of the helix and appear to be only partially ordered. We cannot discern whether the residues are truly less ordered or the NOE data concerning these residues are relatively sparse, partly due to poor resolution in the NMR spectrum.

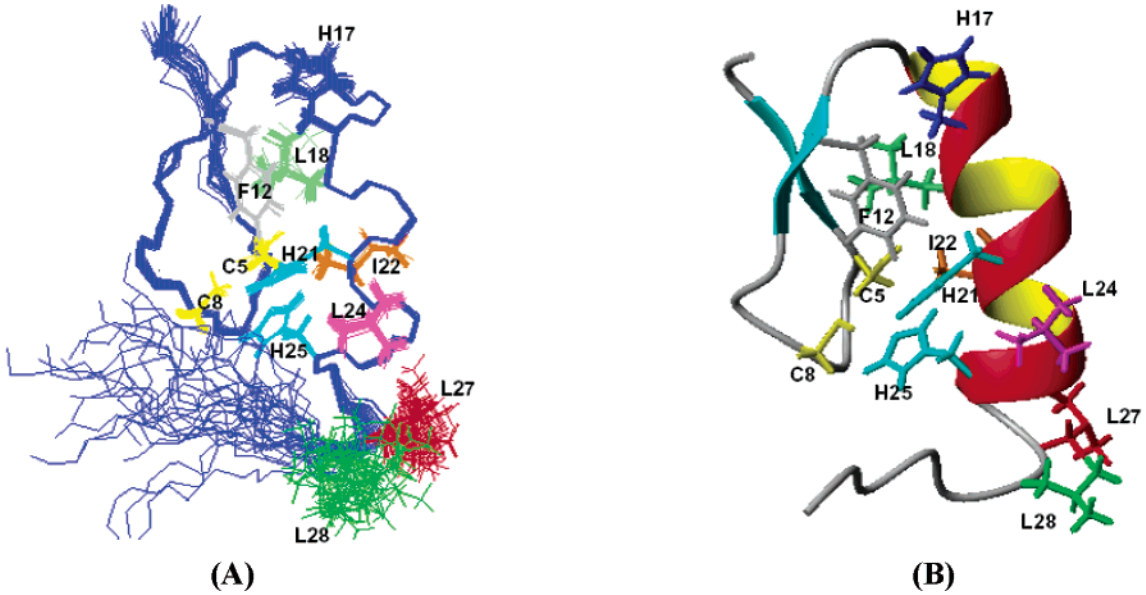

FIGURE 8: Three-dimensional structure of the E6apc2 peptide. (A) Bundle of 30 structures superimposed on the backbone atoms of residues from Phe3 to Glu26. (B) Randomly chosen structure. Side-chains are shown for residues important for forming a stable core or for binding to E6 and are labeled as in Figure 7, except that Leu20, 23, and 24 now appear as Leu24, 27, and 28.

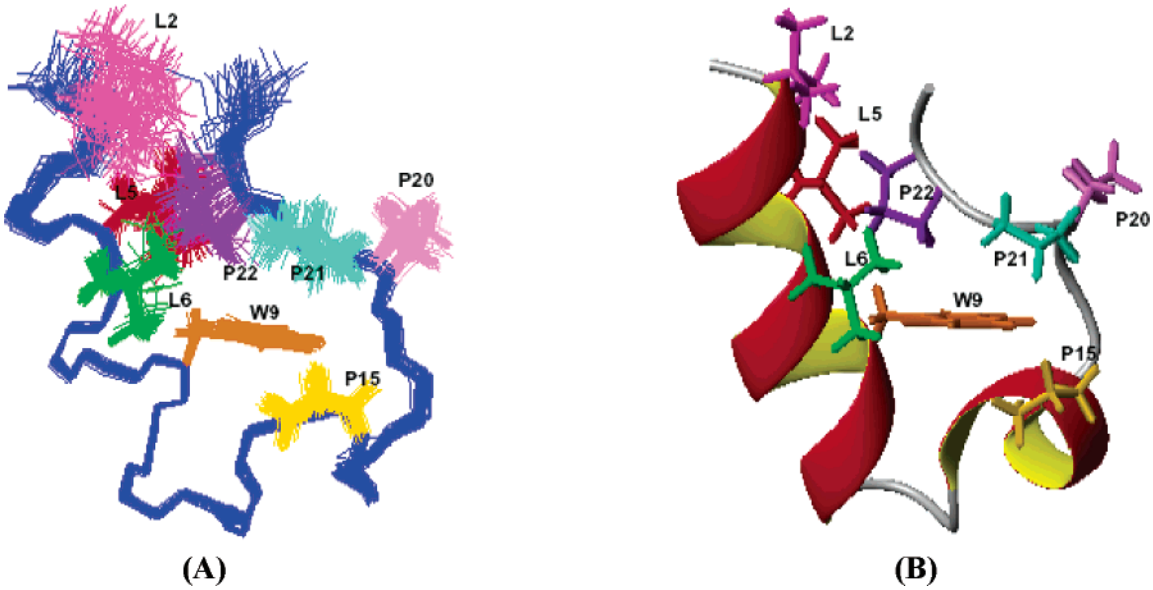

FIGURE 9: Three-dimensional structure of the E6apn1 peptides. (A) Bundle of 50 structures superimposed on backbone atoms of residues Gln3 to Pro20. (B) Randomly chosen structure. Side-chains are labeled for residues important for forming a stable core (Trp9 is dark orange; Pro15 is red; and Pro22 is violet) or for binding to E6 (Leu2 is magenta; Leu5 is red; and Leu6 is green).

Peptide E6apn1 forms a globular structure through hydrophobic interactions between Trp9 and Leu6, Pro15, Pro21, and Pro22 (Figure 9). Trp9 is located at the center of a hydrophobic core and makes contacts similar to those in the original 20 amino acid peptide reported by Neidigh et al. (*34*). Residues 2−11 and 14−17 form two α-helices. The three leucine residues of the assumed binding motif are at positions 2, 5, and 6, respectively, at the beginning of the first α-helix. Their side-chains partially extend into the interior of the peptide.

DISCUSSION

Comparison of the E6apc1 and E6apc2 structures with that of the parent zinc finger (1SP1) showed that the scaffold structure is unperturbed according to four criteria: (1) Low rms deviation of superimposed atoms, (2) similar torsion angles (3) similar hydrogen bonding patterns, and (4) similar global structures. (1) The rms deviations of 1SP1 with E6apc1 and E6apc2 after superimposing the backbone atoms for residues 3−25 were 1.0 and 1.2 Å, respectively; that of the helices encompassing residues 15−25 are just 0.4 and 1.0 Å, respectively. (The rms deviation between E6apc1 and E6apc2 for residues 3−25 is 1.2 Å.) (2) The backbone φ and ψ angles of residues 3−25 were not significantly different among the structures. (3) Both 1SP1 and E6apc2 have the regular CO_i-NH_{i+4} hydrogen bond pattern expected for α-helices, as observed in the parent E6ap18 peptide that we studied earlier (*26*). Interestingly, for E6apc1, residues 15−22 possess the typical α-helical CO_i-NH_{i+4} hydrogen bonds, whereas the HN of residues 23−25 participate in CO_i-NH_{i+3} H-bonds typical of 3_{10} helix. The majority of calculated structures also show a Leu23 CO to Asn27 NH hydrogen bond, which hints that the middle of the helix in

E6apc1 is more compact than a regular α-helix. (4) Distance difference matrix (DDM) analyses were used to provide information about the relative disposition of the backbone atoms in the structures. It is an effective approach to compare structures of the same protein or of homologous proteins (*52*, *53*). The α-carbon DDM plots of residues 3−25 showed that there are no significant distance changes (<2 Å) in the three structures. In summary, the E6apc peptides and the zinc finger scaffold all have similar overall structures and differ only whether they contain the residues of the E6-binding motif and how the side-chains of these residues are presented.

Comparison of the E6apn1 structure with that of the parent Trp-cage peptide also showed that the scaffold structure is unperturbed. The backbone rms deviation of Trp-cage (residues 2−20) with the corresponding residues of E6apn1 (residues 5−23) is only 0.6 Å. The hydrogen bonding pattern in the helices of E6apn1 was also analyzed, and as in 1SP1, CO_i-NH_{i+4} hydrogen bonds were found. On the whole, the ϕ and ψ angles of E6apn1 and Trp-cage are the same. A difference was noted for the $\chi1$ angle of Ser17, which is 75 ± 29 in E6apn1 and −58 ± 37 for the corresponding residue of Trp-cage (Ser14). Two small (<6 Hz) $^3J_{\alpha\beta2}$ and $^3J_{\alpha\beta3}$ coupling constants support a $\chi1$ angle of around +60° in E6apn1. (The gauche$^+$ conformation Ser17 may be important to allow formation of the hydrogen bond between Gly14 CO and Ser17 NH that was observed in 49 of 50 calculated structures of E6apn1.) The α-carbon DDM plots showed that for the well-structured regions, the distance differences were much smaller than 2 Å; most were in the range of 0−1 Å.

We have therefore successfully grafted the E6-binding motif into two parent peptides while preserving the structure of their scaffolds. The presence of similar structural platforms facilitates discussion of flexibility. In E6apc1, the backbone atoms of the three key leucine residues are fixed in the compact helix, while their side-chains extend outside. The exposure of these residues should facilitate binding to E6. The absence of inhibitory activity, coupled with the observation of the available but fixed helical conformation of the three leucine residues, suggests that the conformation of the peptide cannot match the binding site in E6 protein. In E6apc2, the key leucine residues are shifted by three amino acid residues (about one turn of the helix) toward the C-terminus. The leucine side-chains also extend outside and are available to bind to E6 with even less spatial encumbrance than in E6apc1. Because both peptides retain the histidine and cysteine residues that coordinate Zn^{2+}, changes in metal ion binding and associated changes in structures are unlikely to be the reasons E6apc1 loses activity and E6apc2 exhibits it. One hypothesis is that the flexible C-terminus of E6apc2 allows it to possess activity, whereas the relatively fixed C-terminus of E6apc1 does not allow activity. The results from the short, flexible peptides E6apm (8 amino acid residues) and E6ap18 (18 amino acid residues) support this hypothesis. E6ap18, which adopts a fluctuating α-helix structure in aqueous buffer (*26*) that is corroborated by recent molecular dynamics simulation data (*54*), possesses inhibition activity. The unstructured short peptide E6apm can also inhibit the E6−E6AP interaction. On the other hand, the structure of E6apn1 argues that flexibility at the C-terminus of the E6-binding motif may not be a requirement. In E6apn1, the two C-terminal leucine resides of the E6-binding motif are in an α-helical conformation, yet the peptide still inhibits the E6−E6AP interaction. However, because the thermal unfolding of E6apn1 indicates that its structure is only marginally stable (and much less stable than that of E6apc1), the E6apn1 peptide may undergo significant conformational change upon binding to E6 without a large energetic penalty. Even at 7 °C where the NMR spectra for the structure were acquired, the E6apn1 peptide is approximately 10% unfolded according to the CD data (Figure 4B). Therefore, the structure of this peptide is unlikely to be rigid even at 4 °C where the binding assay is performed. The lack of a fluctuating conformation may not be the only reason E6apc1 loses its inhibition activity: an alternative explanation is that the small residue, which is replaced by His25 in E6apc1, is required, not just preferred, in the consensus binding motif (LxxϕLsh). Replacement of the small amino acid (identified only by consensus among E6 binding proteins) with histidine in other E6-binding peptides could be used to test this hypothesis. In addition, we have little information on the conformational preferences of the glycine-glutamate portion at the C-terminal end of the motif. Nonetheless, the summary result from this study is that a portion of the E6ap motif binds E6 by a regular helical motif, which is supported by a recent study that examined a related family of E6-inhibitory peptides (*37*).

Assuming that the E6apm peptide binds to E6 with a helix similar to that of the other peptides, a large conformational change must be induced. The conformation of the peptide while bound to E6 would give a precise definition of the conformational changes that accompany binding, which can be determined by transferred NOE experiments. However, recombinant soluble and stable high-risk E6 has not been readily available (*5*, *39*, *40*), precluding those kinds of experiments from being performed.

Conformational changes in all the peptides must be required for binding E6. For example, in the E6apn1 structure, the side-chains of the key "E6-binding" Leu5 and Leu6 residues extend inside the structure, sandwiching Pro22 between them. The side-chain of Leu6 also contacts the side-chain of Trp9 in a hydrophobic interaction. A similar phenomenon was observed in the structure of another E6-binding peptide, E6bp, for which the side-chains of the three key hydrophobic residues also reside inside the structure, in this case forming part of a dimer interface (*27*, unpublished results). One explanation is that the leucines interact to stabilize the internal structure of E6AP and the binding to E6 actually occurs on the opposite face. The mutagenesis data argue against this hypothesis because replacing even a single leucine does not appreciably change the structure (*26*) but abrogates binding, whereas mutagenesis of residues on the opposite face has much less of an effect. A more likely explanation is that recognition of E6ap to E6 protein is not executed by one step involving the three key, hydrophobic leucine residues but includes two or more steps. First, there must be one or more residues that interact with E6 protein to induce a conformational change that exposes the leucine residues and matches the binding interface. Further research is needed to investigate which residue (or residues) in the consensus motif makes the initial contact and how a subsequent conformational change matches the binding of E6ap with E6 protein.

Our previous report showed that an 18 amino acid residue peptide containing the E6-binding consensus region possesses

significant α-helical conformation only in the presence of more than 30% TFE (*26*). Because TFE is an α-helix promoter (*26*, *55*−*57*), the structures determined in TFE solution must be interpreted with caution. The structures of the peptides described here in aqueous solution without TFE are more likely to mimic the native states in the absence of the binding partner E6 protein. By restricting the binding domain in various helical conformations and measuring changes in biological activity, it may be possible to sample the biologically relevant states in the presence of the binding partner E6 protein. Further design of these peptides will be enhanced by knowing the precise three-dimensional bound conformation that shows the hydrophobic groups, hydrogen bonding patterns, and salt-bridge interactions important for the peptide−protein interface, which cannot be mimicked by determining structures in TFE.

We found that one-shot protein grafting can be used to create monomeric E6-binding ligands that are structurally stable. The conformational analysis presented here suggests that the E6-binding motif in these scaffolds can be optimized further using peptide display methods or limited mutagenesis. The characterization of such biologically active ligands will help their definition, thus aiding the design of future peptides and nonpeptidic low molecular weight compounds. The strategies used here are immediately applicable to the design of inhibitors for proteins similar to E6 that use binding pockets that bind helical peptides such as the HIV-1 gp41 protein, the antiapoptotic Bcl proteins, and the P53-binding MDM2 protein (*45*, *58*, *59*).

ACKNOWLEDGMENT

We thank Dr. James Sudmeier for help with setting up NMR experiments and Matthew Fesinmeyer and Dr. Neils Andersen for protocols and discussion of the Trp-cage structure.

SUPPORTING INFORMATION AVAILABLE

Three figures showing representative NMR data and three tables of chemical shift assignments. This material is available free of charge via the Internet at http://pubs.acs.org.

REFERENCES

1. zur Hausen, H. (1991) Human papillomaviruses in the pathogenesis of anogenital cancer. *Virology 184*, 9−13.
2. Scheffner, M., Huibregtse, J. M., and Howley, P. M. (1994) Identification of a human ubiquitin-conjugating enzyme that mediates the E6-AP-dependent ubiquitination of p53. *Proc. Natl. Acad. Sci. U.S.A. 91*, 8797−8801.
3. Barbosa, M. S., Lowy, D. R., and Schiller, J. T. (1989) Papillomavirus polypeptides E6 and E7 are zinc-binding proteins. *J. Virol. 63*, 1404−1407.
4. Grossman, S. R. and Laimins, L. A. (1989) E6 protein of human papillomavirus type 18 binds zinc. *Oncogene 4*, 1089−1093.
5. Lipari, F., McGibbon, G. A., Wardrop, E., and Cordingley, M. G. (2001) Purification and biophysical characterization of a minimal functional domain and of an N-terminal Zn2+-binding fragment from the human papillomavirus type 16 E6 protein. *Biochemistry 40*, 1196−1204.
6. Ristriani, T., Nomine, Y., Masson, R., Weiss, E., and Trave, G. (2001) Specific recognition of four-way DNA junctions by the C-terminal zinc-binding domain of HPV oncoprotein E6. *J. Mol. Biol. 305*, 729−739.
7. Scheffner, M., Werness, B. A., Huibregtse, J. M., Levine, A. J., and Howley, P. M. (1990) The E6 oncoprotein encoded by human papillomavirus types 16 and 18 promotes the degradation of p53. *Cell 63*, 1129−1136.
8. Huibregtse, J. M., Scheffner, M., and Howley, P. M. (1994) E6-AP directs the HPV E6-dependent inactivation of p53 and is representative of a family of structurally and functionally related proteins. *Cold Spring Harb. Symp. Quant. Biol. 59*, 237−245.
9. Scheffner, M., Huibregtse, J. M., Vierstra, R. D., and Howley, P. M. (1993) The HPV-16 E6 and E6-AP complex functions as a ubiquitin-protein ligase in the ubiquitination of p53. *Cell 75*, 495−505.
10. Chen, J. J., Reid, C. E., Band, V., and Androphy, E. J. (1995) Interaction of papillomavirus E6 oncoproteins with a putative calcium-binding protein. *Science 269*, 529−531.
11. Du, M., Fan, X., Hong, E., and Chen, J. J. (2002) Interaction of oncogenic papillomavirus E6 proteins with fibulin-1. *Biochem. Biophys. Res. Commun. 296*, 962−969.
12. Zimmermann, H., Koh, C. H., Degenkolbe, R., O'Connor, M. J., Muller, A., Steger, G., Chen, J. J., Lui, Y., Androphy, E., and Bernard, H. U. (2000) Interaction with CBP/p300 enables the bovine papillomavirus type 1 E6 oncoprotein to downregulate CBP/p300-mediated transactivation by p53. *J. Gen. Virol. 81*, 2617−2623.
13. Degenhardt, Y. Y. and Silverstein, S. (2001) Interaction of zyxin, a focal adhesion protein, with the E6 protein from human papillomavirus type 6 results in its nuclear translocation. *J. Virol. 75*, 11791−11802.
14. Thomas, M., Glaunsinger, B., Pim, D., Javier, R., and Banks, L. (2001) HPV E6 and MAGUK protein interactions: determination of the molecular basis for specific protein recognition and degradation. *Oncogene 20*, 5431−5439.
15. Kiyono, T., Hiraiwa, A., Fujita, M., Hayashi, Y., Akiyama, T., and Ishibashi, M. (1997) Binding of high-risk human papillomavirus E6 oncoproteins to the human homologue of the Drosophila discs large tumor suppressor protein. *Proc. Natl. Acad. Sci. U.S.A. 94*, 11612−11616.
16. Vande Pol, S. B., Brown, M. C., and Turner, C. E. (1998) Association of Bovine Papillomavirus Type 1 E6 oncoprotein with the focal adhesion protein paxillin through a conserved protein interaction motif. *Oncogene 16*, 43−52.
17. Tong, X., Salgia, R., Li, J. L., Griffin, J. D., and Howley, P. M. (1997) The bovine papillomavirus E6 protein binds to the LD motif repeats of paxillin and blocks its interaction with vinculin and the focal adhesion kinase. *J. Biol. Chem. 272*, 33373−33376.
18. Tong, X., Boll, W., Kirchhausen, T., and Howley, P. M. (1998) Interaction of the bovine papillomavirus E6 protein with the clathrin adaptor complex AP-1. *J. Virol. 72*, 476−482.
19. Thomas, M. and Banks, L. (1999) Human papillomavirus (HPV) E6 interactions with Bak are conserved amongst E6 proteins from high and low risk HPV types. *J. Gen. Virol. 80*, 1513−1517.
20. Thomas, M. and Banks, L. (1998) Inhibition of Bak-induced apoptosis by HPV-18 E6. *Oncogene 17*, 2943−2954.
21. Gao, Q., Srinivasan, S., Boyer, S. N., Wazer, D. E., and Band, V. (1999) The E6 oncoproteins of high-risk papillomaviruses bind to a novel putative GAP protein, E6TP1, and target it for degradation. *Mol. Cell Biol. 19*, 733−744.
22. Li, S., Labrecque, S., Gauzzi, M. C., Cuddihy, A. R., Wong, A. H., Pellegrini, S., Matlashewski, G. J., and Koromilas, A. E. (1999) The human papilloma virus (HPV)-18 E6 oncoprotein physically associates with Tyk2 and impairs Jak-STAT activation by interferon-alpha. *Oncogene 18*, 5727−5737.
23. Nakagawa, S. and Huibregtse, J. M. (2000) Human scribble (Vartul) is targeted for ubiquitin-mediated degradation by the high-risk papillomavirus E6 proteins and the E6AP ubiquitin-protein ligase. *Mol. Cell Biol. 20*, 8244−8253.
24. Filippova, M., Song, H., Connolly, J. L., Dermody, T. S., and Duerksen-Hughes, P. J. (2002) The human papillomavirus 16 E6 protein binds to tumor necrosis factor (TNF) R1 and protects cells from TNF-induced apoptosis. *J. Biol. Chem. 277*, 21730−21739.
25. Ristriani, T., Masson, M., Nomine, Y., Laurent, C., Lefevre, J. F., Weiss, E., and Trave, G. (2000) HPV oncoprotein E6 is a structure-dependent DNA-binding protein that recognizes four-way junctions. *J. Mol. Biol. 296*, 1189−1203.
26. Be, X., Hong, Y., Wei, J., Androphy, E. J., Chen, J. J., and Baleja, J. D. (2001) Solution structure determination and mutational analysis of the papillomavirus E6 interacting peptide of E6AP. *Biochemistry 40*, 1293−1299.
27. Chen, J. J., Hong, Y., Rustamzadeh, E., Baleja, J. D., and Androphy, E. J. (1998) Identification of an alpha helical motif sufficient for association with papillomavirus E6. *J. Biol. Chem. 273*, 13537−13544.

28. Bohl, J., Das, K., Dasgupta, B., and Vande Pol, S. B. (2000) Competitive binding to a charged leucine motif represses transformation by a papillomavirus E6 oncoprotein. *Virology 271*, 163−170.
29. Hoellerer, M. K., Noble, M. E., Labesse, G., Campbell, I. D., Werner, J. M., and Arold, S. T. (2003) Molecular recognition of paxillin LD motifs by the focal adhesion targeting domain. *Structure 11*, 1207−1217.
30. Wright, P. E. and Dyson, H. J. (1999) Intrinsically unstructured proteins: re-assessing the protein structure−function paradigm. *J. Mol. Biol. 293*, 321−331.
31. Bohm, G., Muhr, R., and Jaenicke, R. (1992) Quantitative analysis of protein far UV circular dichroism spectra by neural networks. *Protein Eng. 5*, 191−195.
32. Cavanagh, J. (1996) *Protein NMR Spectroscopy: Principles and Practice* Academic Press, San Diego.
33. Wüthrich, K. (1986) *NMR of Proteins and Nucleic Acids* Wiley, New York.
34. Neidigh, J. W., Fesinmeyer, R. M., and Andersen, N. H. (2002) Designing a 20-residue protein. *Nat. Struct. Biol. 9*, 425−430.
35. Neidigh, J. W., Fesinmeyer, R. M., Prickett, K. S., and Andersen, N. H. (2001) Exendin-4 and glucagon-like-peptide-1: NMR structural comparisons in the solution and micelle-associated states. *Biochemistry 40*, 13188−13200.
36. Koradi, R., Billeter, M., and Wüthrich, K. (1996) MOLMOL: a program for display and analysis of macromolecular structures. *J. Mol. Graph. 14*, 51−55.
37. Sterlinko Grm, H., Weber, M., Elston, R., McIntosh, P., Griffin, H., Banks, L., and Doorbar, J. (2004) Inhibition of E6-induced degradation of its cellular substrates by novel blocking peptides. *J. Mol. Biol. 335*, 971−985.
38. Nomine, Y., Ristriani, T., Laurent, C., Lefevre, J. F., Weiss, E., and Trave, G. (2001) Formation of soluble inclusion bodies by HPV E6 oncoprotein fused to maltose-binding protein. *Protein Expression Purif. 23*, 22−32.
39. Nomine, Y., Ristriani, T., Laurent, C., Lefevre, J. F., Weiss, E., and Trave, G. (2001) A strategy for optimizing the monodispersity of fusion proteins: application to purification of recombinant HPV E6 oncoprotein. *Protein Eng. 14*, 297−305.
40. Degenkolbe, R., Gilligan, P., Gupta, S., and Bernard, H. U. (2003) Chelating agents stabilize the monomeric state of the zinc binding human papillomavirus 16 E6 oncoprotein. *Biochemistry 42*, 3868−3873.
41. Narayan, V. A., Kriwacki, R. W., and Caradonna, J. P. (1997) Structures of zinc finger domains from transcription factor Sp1. Insights into sequence-specific protein−DNA recognition. *J. Biol. Chem. 272*, 7801−7809.
42. Kriwacki, R. W., Schultz, S. C., Steitz, T. A., and Caradonna, J. P. (1992) Sequence-specific recognition of DNA by zinc-finger peptides derived from the transcription factor Sp1. *Proc. Natl. Acad. Sci. U.S.A. 89*, 9759−9763.
43. Frankel, A. D., Berg, J. M., and Pabo, C. O. (1987) Metal-dependent folding of a single zinc finger from transcription factor IIIA. *Proc. Natl. Acad. Sci. U.S.A. 84*, 4841−4845.
44. Kuwahara, J. and Coleman, J. E. (1990) Role of the zinc(II) ions in the structure of the three-finger DNA binding domain of the Sp1 transcription factor. *Biochemistry 29*, 8627−8631.
45. Sia, S. K., Carr, P. A., Cochran, A. G., Malashkevich, V. N., and Kim, P. S. (2002) Short constrained peptides that inhibit HIV-1 entry. *Proc. Natl. Acad. Sci. U.S.A. 99*, 14664−14669.
46. Arumugam, S., Gao, G., Patton, B. L., Semenchenko, V., Brew, K., and Van Doren, S. R. (2003) Increased backbone mobility in beta-barrel enhances entropy gain driving binding of N-TIMP-1 to MMP-3. *J. Mol. Biol. 327*, 719−734.
47. Merutka, G., Dyson, H. J., and Wright, P. E. (1995) Random coil H-1 chemical-shifts obtained as a function of temperature and trifluoroethanol concentration for the peptide series GGXGG. *J. Biomol. NMR 5*, 14−24.
48. Wishart, D. S., Bigam, C. G., Yao, J., Abildgaard, F., Dyson, H. J., Oldfield, E., Markley, J. L., and Sykes, B. D. (1995) H-1, C-13 and N-15 chemical-shift referencing in biomolecular NMR. *J. Biomol. NMR 6*, 135−140.
49. Hyberts, S. G., Goldberg, M. S., Havel, T. F., and Wagner, G. (1992) The solution structure of eglin c based on measurements of many NOEs and coupling constants and its comparison with X-ray structures. *Protein Sci. 1*, 736−751.
50. Szyperski, T., Guntert, P., and Otting, G. (1992) Determination of Scalar Coupling-Constants by Inverse Fourier Transformation of In-Phase Multiplets. *J. Magn. Reson. 99*, 552−560.
51. Mayer, K. L. and Stone, M. J. (2000) NMR solution structure and receptor peptide binding of the CC chemokine eotaxin-2. *Biochemistry 39*, 8382−8395.
52. Akke, M., Forsen, S., and Chazin, W. J. (1995) Solution structure of (Cd2+)1-calbindin D9k reveals details of the stepwise structural changes along the Apo→(Ca2+)II1→(Ca2+)I,II2 binding pathway. *J. Mol. Biol. 252*, 102−121.
53. Paakkonen, K., Annila, A., Sorsa, T., Pollesello, P., Tilgmann, C., Kilpelainen, I., Karisola, P., Ulmanen, I., and Drakenberg, T. (1998) Solution structure and main chain dynamics of the regulatory domain (residues 1−91) of human cardiac troponin C. *J. Biol. Chem. 273*, 15633−15638.
54. Cui, B., Shen, M. Y., and Freed, K. F. (2003) Folding and misfolding of the papillomavirus E6 interacting peptide E6ap. *Proc. Natl. Acad. Sci. U.S.A. 100*, 7087−7092.
55. Luidens, M. K., Figge, J., Breese, K., and Vajda, S. (1996) Predicted and trifluoroethanol-induced alpha-helicity of polypeptides. *Biopolymers 39*, 367−376.
56. Main, E. R. and Jackson, S. E. (1999) Does trifluoroethanol affect folding pathways and can it be used as a probe of structure in transition states? *Nat. Struct. Biol. 6*, 831−835.
57. Ionescu, R. M. and Matthews, C. R. (1999) Folding under the influence. *Nat. Struct. Biol. 6*, 304−307.
58. Vassilev, L. T., Vu, B. T., Graves, B., Carvajal, D., Podlaski, F., Filipovic, Z., Kong, N., Kammlott, U., Lukacs, C., Klein, C., Fotouhi, N., and Liu, E. A. (2004) In vivo activation of the p53 pathway by small-molecule antagonists of MDM2. *Science 303*, 844−848.
59. Rutledge, S. E., Volkman, H. M., and Schepartz, A. (2003) Molecular recognition of protein surfaces: high affinity ligands for the CBP KIX domain. *J. Am. Chem. Soc. 125*, 14336−14347.

BI049552A